Opto-Electronic Advances

Review

2019, Vol. 2, No. 10

DOI: 10.29026/oea.2019.190011

A review on control methodologies of disturbance rejections in optical telescope

Tao Tang[1,2], Shuaixu Niu[1,2,3], Jiaguang Ma[1,2], Bo Qi[1,2]*, Ge Ren[1,2], and Yongmei Huang[1,2]

Structural vibrations in Tip-Tilt modes usually affect the closed-loop performance of astronomically optical telescopes. In this paper, the state of art control methods—proportional integral (PI) control, linear quadratic Gaussian (LQG) control, disturbance feed forward (DFF) control, and disturbance observer control (DOBC) of Tip-Tilt mirror to reject vibrations are first reviewed, and then compared systematically and comprehensively. Some mathematical transformations allow PI, LQG, DFF, and DOBC to be described in a uniform framework of sensitivity function that expresses their advantages and disadvantages. In essence, feed forward control based-inverse model is the main idea of current techniques, which is dependent on accuracies of models in terms of Tip-Tilt mirror and vibrations. DOBC can relax dependences on accuracy model, and therefore this survey concentrates on concise tutorials of this method with clear descriptions of their features in the control area of disturbance rejections. Its applications in various conditions are reviewed with emphasis on the effectiveness. Finally, the open problems, challenges and research prospects of DOBC of Tip-Tilt mirror are discussed.

Keywords: structural vibrations; astronomical telescope; Q-filter; error-based DOBC; Tip-Tilt mirror

Tang T, Niu S X, Ma J G, Qi B, Ren G *et al*. A survey on control methodologies of disturbance rejections in optical telescope. *Opto-Electron Adv* **2**, 190011 (2019).

Introduction

Disturbance rejection is one of the hottest topics in the high-performance servoing control areas[1–5]. Optical telescopes also face this issue, because the telescopes' imaging quality and their ability to observe faint stars at the diffraction limit is limited by the disturbances induced by wind shaking, equipment vibration and platform vibration[6–10]. High control bandwidth is the simplest method to reject vibrations. However, long integration time of the image sensor is always required for a high signal to noise, which restricts the closed-loop control bandwidth. Therefore, the vibrations induced by telescope structures could not be fully compensated by classical control loops[11,12]. If disturbances are measurable, it is obvious that a disturbance feedforward control strategy is the most effective way to attenuate them[13–15]. Although the structural vibrations can be directly measured by extra inertial sensors, it is difficult to extract useful information to control the Tip-Tilt mirror. Furthermore, the estimation accuracy of disturbance using inertial sensors is affected by random drifting. To overcome these difficulties, one intuitive idea (called based-model control) for estimating disturbances through known variables to reject vibration is proposed, such that the disturbances can be compensated by the estimations rather than other sensors. These based-model control techniques are attractive in many practical scenarios, such as spacecraft, airplanes, vehicles and other platforms, due to its simplification and effectiveness. Related works are organized as follows. Frequency-based design of Modal-Control[16] is presented to reduce the effects of distortions in ground-based telescopes. Simulations show that the proposed approach is a promising technique to improve the performance of the closed-loop control system. An adaptive control algorithm[17,18] to reject vibrations is developed and adapted to the complex control architectures. This adaptive vibration cancellation algorithm was integrated into a telescope

[1]Institute of Optics and Electronics, Chinese Academy of Sciences, Chengdu 610209, China; [2]Key Laboratory of Optical Engineering, Chinese Academy of Sciences, Chengdu 610209, China; [3]University of Chinese Academy of Sciences, Beijing 100049, China.
*Correspondence: B Qi, E-mail: qibo@ioe.ac.cn
Received: 1 March 2019; Accepted: 25 June 2019; Published: 18 October 2019

currently operating at the European Southern Observatory in Chile and verified experimentally. Recently, some popular controllers focusing on Linear Quadratic Gaussian (LQG) control laws or using H_∞/H_2 synthesis methods[19–22] have been successfully implemented. Existing experiments demonstrate that LQG control can achieve better on-sky performance than a feedback integrator controller in the condition of the optimally identified process model. As far as these techniques are concerned, the control model and the disturbance model play a crucial role in the Tip-Tilt control system. Large model errors usually deteriorate the closed-loop performance, and evenly cause the instability of the control system. Therefore, model identification is the priority when these methods are deployed. Although the control model of the Tip-Tilt mirror exhibits good linearity in the low-frequency domain, the middle-frequency or high-frequency nonlinearities and dynamics cause difficulties in model identification, resulting in hindering to reject the middle-frequency or high-frequency disturbance.

To relax these conditions, the disturbance observer control[23–27] is reviewed and discussed for Tip-Tilt mirror control system in this paper. Furthermore, the error-based DOBC controller[28–31] of Tip-Tilt mirror only based on CCD is proposed here. It can be plugged into an existing feedback loop that leads to a generalized version of 1–Q (Q is the designed filter) brought in the numerator of the original sensitivity function, resulting in the overall sensitivity function equal to zero in theory at the expected frequencies. To suppress different kinds of vibrations, relevant new Q-filters are also optimized to reject low-frequency and high-frequency disturbances. In frequency domain, the error-based DOBC with the improved Q-filters are analyzed in details, and its design procedure and implementation are also introduced. The remainder of this paper is arranged as follows: firstly we present a detailed introduction to conventional proportional integral (PI) control of the Tip-Tilt mirror and give a brief introduction to LQG controller as well as disturbance feedforward (DFF) controller. Secondly, the new error-based DOBC is proposed, which analyzes its characteristics, gives design process, and also sets up simulations and experiments to testify the error-based DOBC of Tip-Tilt mirror. And then, a new repetitive control[32–34] based DOBC is proposed. Eventually, we give the conclusions.

Conventional control of Tip-Tilt mirror

The optical configuration of the Tip-Tilt mirror system[28,29] in the astronomical telescope is illustrated in Fig. 1(a), mainly including image sensor, splitter mirror, control unit, Tip-Tilt mirror, adaptive mirror, and image processing unit. The image sensor can detect the Tip-Tilt error caused by the telescope's structural vibrations. The classical control structure of the Tip-Tilt mirror is briefly demonstrated in Fig. 1(b).

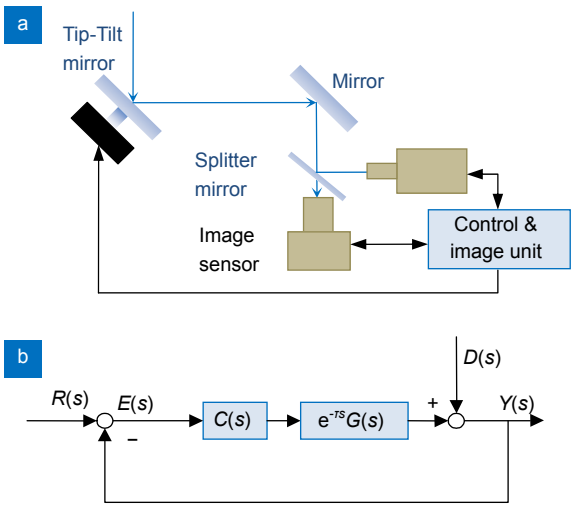

Fig. 1 | Schematic view of the Tip-Tilt mirror system. (a) Typical configuration of Tip-Tilt mirror system. (b) A typical control structure.

$G(s)$ is the controlled plant, and $C(s)$ is the PI controller. The time delay $e^{-\tau s}$ represents the time delay of the control system. $D(s)$ represents the disturbances. $R(s)$ is the target trajectory, and $Y(s)$ is the output. $E(s)$ is the Tip-Tilt error provided by the image sensor. The close-loop error attenuation function $S'_R(s)$ and disturbance attenuation function $S'_D(s)$ are expressed below respectively.

$$S'_R(s)=\frac{E(s)}{R(s)}=\frac{1}{1+C(s)G(s)e^{-\tau s}}\quad , \tag{1}$$

$$S'_D(s)=\frac{Y(s)}{D(s)}=\frac{1}{1+C(s)G(s)e^{-\tau s}}\quad . \tag{2}$$

The Tip-Tilt mirror open-loop nominal response can be expressed as follows

$$G(s)=\frac{1}{\frac{s^2}{\omega_n^2}+2\frac{\xi}{\omega_n}s+1}\frac{1}{T_e s+1}\quad . \tag{3}$$

The natural frequency of Tip-Tilt mirror is usually up to kHz, and the damping factor ξ is much smaller than 1, leading to $G(s)\approx(T_e s+1)^{-1}$. If the resonance frequency is low, a control strategy based on zero-pole cancellation[35] is proposed to extend control bandwidth due to the stability of mechanical characteristic. Defining w_c as the crossover frequency and w_g as the gain frequency of the open-loop transfer function $G_{open}(s)=C(s)\,G(s)$, Eq. (4) can be obtained according to the definition of phase margin and gain margin

$$\begin{cases}\arg[P(jw_c)]\geq\dfrac{\pi}{4}, & |P(jw_c)|=1\\ -20\lg|P(jw_g)|\geq 6, & \arg[P(jw_g)]=-\pi\end{cases}\quad . \tag{4}$$

Based on Eq. (4), we can derive that $w_c=\pi/4\tau$ and $w_g=\pi/2\tau$. As a result, the controller can be expressed as follows:

$$C(s)=\frac{\pi}{4\tau}\frac{T_e s+1}{s} \quad . \tag{5}$$

This controller can stabilize the plant with phase margin no less than 45 degrees and magnitude margin more than 6 dB. Substituting Eq. (5) into Eq. (1), we can have

$$\hat{S}\approx\frac{1}{1+\frac{\pi}{4\tau}\frac{1}{s}e^{-\tau s}} \quad . \tag{6}$$

From Eq. (6), $\left|\hat{S}(jw)\right|_{w=w_c}=\sqrt{2}/2$ results in $w_c\approx\pi\sqrt{2}/(4\tau)$, which is the bandwidth of sensitivity function. Thus, the control performance of the Tip-Tilt mirror is restricted by the time delay of the image sensor.

Linear quadratic Gaussian (LQG) controller

From above analysis, the closed-loop performance is restricted by linear PI controller due to a low bandwidth. For a linear control system driven by additive white Gaussian noise, the linear-quadratic-Gaussian (LQG) control problem[36,37] is to determine an optimal control law in the sense of minimizing the expected errors. The basic LQG control structure of Tip-Tilt mirror is depicted in Fig. 2.

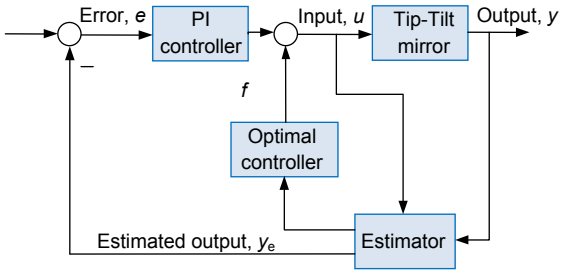

Fig. 2 | LQG control structure of Tip-Tilt mirror.

The closed-loop performance of LQG control is dependent on the optimal controller, which is determined by the estimator. The key process in design LQG control is to choose an optimal metric to evaluate the performance. The accuracy of vibrations model plays an important role in the metric. Therefore, many works about LQG controller concentrate on model identifications in the Tip-Tilt control system. Although LQG controller is implemented in discrete-time domain, the closed-loop transfer function of Tip-Tilt mirror with the LQG controller can be obtained easily through bilinear transformation when the optimal controller is determined by the estimator.

Disturbance feed forward (DFF) controller

It is unavoidable for image sensors to induce time delay, resulting in low control bandwidth to limit vibration rejection, so other sensors independent of image sensors are added to measure vibrations directly so that a disturbance feed forward controller is implemented to eliminate vibrations[37]. Firstly, the vibrations are measured by additional inertial sensors such as accelerometers at the telescope structure and the vibrations are reconstructed by established filter techniques. The reconstructed signals are used feedforward for controlling the Tip-Tilt mirror loop. The basic control structure is shown in Fig. 3.

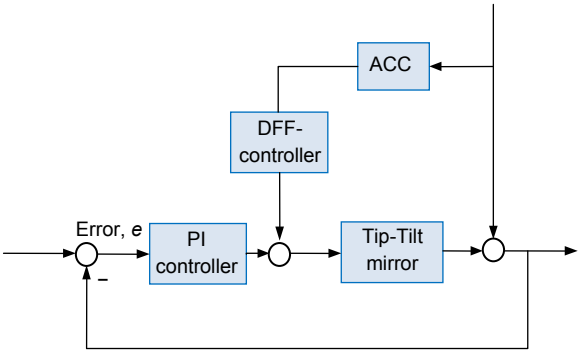

Fig. 3 | DFF control structure of Tip-Tilt mirror.

The transfer function of the Fig. 3 can be derived as follows:

$$Y(s)=\frac{C(s)G(s)e^{-\tau s}}{1+C(s)G(s)e^{-\tau s}}R(s)+\frac{1-DFF(s)G(s)}{1+C(s)G(s)e^{-\tau s}}D(s) \quad . \tag{7}$$

The vibrations can be totally cancelled under the following condition:

$$DFF(s)=\frac{1}{G(s)} \quad . \tag{8}$$

Obviously, this perfect condition cannot be satisfied due to model errors existed in the Tip-Tilt control system. Although the partial compensation of Eq. (8) is effective to low-frequency vibrations, the final performance is directly affected by the reconstructed accuracy of vibrations. In fact, DFF is effective only with vibrations generated by the optical platform. However, these disturbances can occur at any point along the optical link due to structural flexibility, and therefore could not be reconstructed precisely to feedforward control of the Tip-Tilt mirror.

Disturbance observer control (DOBC)

To avoid complexities of extra load on the Tip-Tilt control system, the DOBC is proposed to improve the closed-loop system. In comparisons with LQG controller, this new method can enhance the original PI control system without deteriorating stability. Furthermore, the control system in the DOBC mode can obviously exhibit the open-loop and closed-loop characteristics in frequency domain. Fig. 4 shows the conventional DOBC structure[25,26]. $Q(s)$ is the designed filter. The inverse of the control plant $G(s)$ is described by $G_m^{-1}(s)$. In the image sensor-based control system, the position sensor $Y(s)$ cannot measure the disturbance $D(s)$ directly. Thus, a new control block diagram[29,30] in the presence of the disturbance is proposed in Fig. 5.

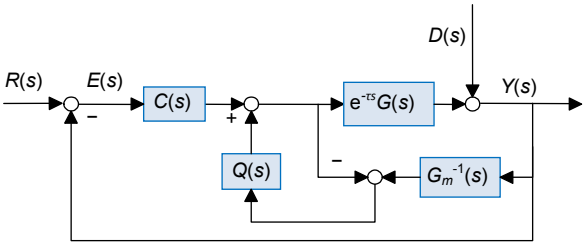

Fig. 4 | Conventional DOBC structure of Tip-Tilt mirror.

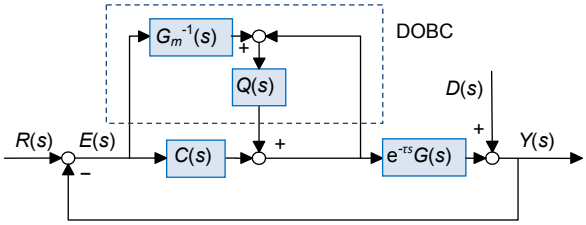

Fig. 5 | Error-based DOBC structure of Tip-Tilt mirror.

The new closed-loop sensitivity transfer functions illustrated in Fig. 5 can be expressed as follows:

$$S_R(s)=\frac{1-Q(s)}{1+C(s)G(s)\mathrm{e}^{-\tau s}+(\mathrm{e}^{-\tau s}G(s)G_m^{-1}(s)-1)Q(s)} \quad (9)$$

$$S_D(s)=\frac{1-Q(s)}{1+C(s)G(s)\mathrm{e}^{-\tau s}+(\mathrm{e}^{-\tau s}G(s)G_m^{-1}(s)-1)Q(s)} \quad . (10)$$

$S_R(s)=[1-Q(s)]S_R'(s)$ and $S_D(s)=[1-Q(s)]S_D'(s)$ can be obtained if $[\mathrm{e}^{-\tau s}G(s)G_m^{-1}(s)-1]Q(s)\approx 0$. In this control mode, the main objective is to make $1-Q(s)$ close to zero at the disturbance frequencies, and meanwhile, not to deteriorate the closed-loop performance of the original control system. The characteristic polynomial $W(s)$ of the closed-loop system can be expressed as

$$W(s)=1+\mathrm{e}^{-\eta s}C(s)\,G(s)+\left(G_m^{-1}(s)\,G(s)-1\right)Q(s)$$

$$=\left(1+\mathrm{e}^{-\eta s}C(s)\,G(s)\right)\left(1+\frac{\left(G_m^{-1}(s)\,G(s)-1\right)Q(s)}{1+\mathrm{e}^{-\eta s}C(s)\,G(s)}\right) \quad , (11)$$

Because the original feedback system is stable, it implies that the stability condition of the closed-loop control system has to satisfy the following condition according to Small Gain Theorem:

$$\left\|\frac{\left(G_m^{-1}(s)\,G(s)-1\right)Q(s)}{1+\mathrm{e}^{-\eta s}C(s)\,G(s)}\right\|_\infty<1 \quad . \quad (12)$$

Frequency based design of Q-filter

Low-pass filter

Without doubt, the Q-filter could be designed as a low-pass filter[26], because the disturbance to be rejected is usually with low or medium frequency, whereas the sensor noise is with medium or high frequency. Therefore, the error-based DOBC is able to estimate the disturbance and uncertainty in a low and medium frequency range but filter out the high-frequency measurement noise. The general form of low-pass filters can be described as follows:

$$Q_L(s)=\frac{\sum_{k=2}^{m-2}C_m^k(\tau s)^k+1}{(\tau s+1)^m} \quad . \quad (13)$$

The general filters of Eq. (13) are subject to the orders of the filter and the time delay. Q_{31}-filter[39,40] is considered as an optimal low-pass filter for the closed-loop performance in terms of bandwidth and robustness. $\tau=15\eta$ is an optimal parameter of Q_{31}-filter to make the phase margin and magnitude margin of the open-loop transfer function being robust.

There is an example of the Tip-Tilt mirror that compares Bode responses of the sensitivity functions in the modes of the PI and the DOBC controller in Fig. 6. The sampling frequency is 2000 Hz, and the time delay approximates with 0.0015. Obviously, Fig. 6 shows that the DOBC controller can achieve an extra improvement below the frequencies of 10 Hz.

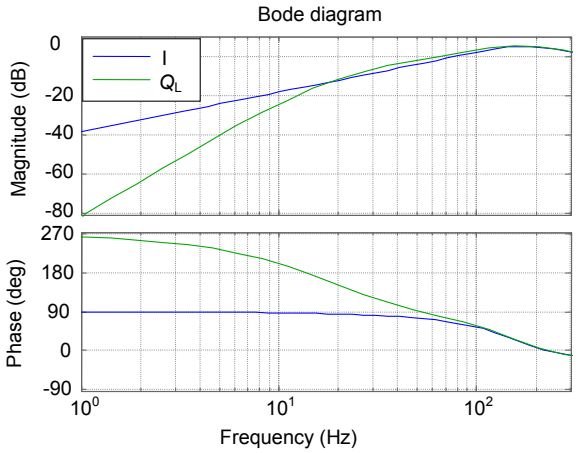

Fig. 6 | Bode response of the sensitivity function with *I* and $Q_L(s)$.

From Fig. 7, the DOBC with the low-pass filter is verified effectively to mitigate the low-frequency disturbances.

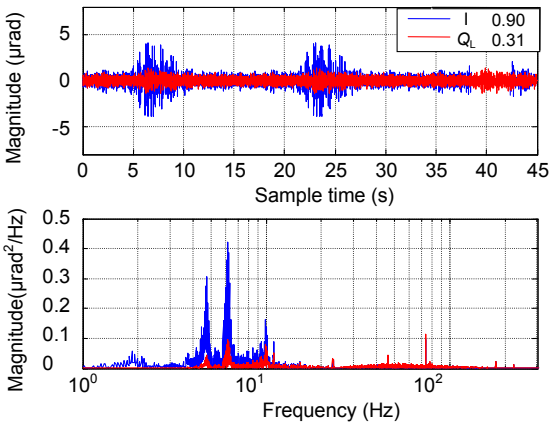

Fig. 7 | The closed-loop Tip-Tilt errors.

Band-pass filter

High rejection bandwidth in the low-pass filter control mode could be limited due to the stability condition of Eq. (8), leading to no mitigation of high-frequency disturbances. To overcome this problem, another way of canceling disturbances[29] is expressed as follows

$$[1-Q(s)]D(s)=0 \quad . \tag{14}$$

Suppose that the disturbance $D(s)$ can be defined as:

$$D(s)=A_i\sum_{i=0}^{k}\varphi(s,w_i) \quad , \tag{15}$$

where w_i is the i-th disturbance with the maximum amplitude of A_i, and $|\varphi(jw,w_i)|\le 1$. When $[1-Q(s)]=\prod_{i=1}^{k}(\frac{s^2}{w_i^2}+1)$, we can derive that

$$[1-Q(s)]D(s)=\prod_{i=1}^{k}(\frac{s^2}{w_i^2}+1)D(s)=0 \quad . \tag{16}$$

The above condition is impractical, because $\prod_{i=1}^{k}(\frac{s^2}{w_i^2}+1)$ is non-causal, and cannot be implemented in a digital control system. A proposed filter to reconstruct Eq. (16) can be designed, and its extra sensitivity functions $ESF(s)$ can be expressed as follows:

$$ESF(s)=1-Q(s)=\prod_{i=1}^{k}\frac{\frac{s^2}{w_i^2}+\zeta_i\frac{s}{w_i}+1}{\frac{s^2}{w_i^2}+\alpha_i\zeta_i\frac{s}{w_i}+\beta_i} \quad , \tag{17}$$

here, the three parameters follow that $\alpha_i>0$, $1>\zeta_i>0$, $\beta_i>0$. With the filter expressed in Eq. (17), disturbances can be reduced approximately to $\sum_{i=0}^{k}A_i/\alpha_i$. $Q(s)$ characterizes a band-pass filter, which can be expressed below.

$$\begin{aligned}Q(s)&=1-\prod_{i=1}^{k}\frac{\frac{s^2}{w_i^2}+\zeta_i\frac{s}{w_i}+1}{\frac{s^2}{w_i^2}+\alpha_i\zeta_i\frac{s}{w_i}+1}\\&=\frac{\prod_{i=1}^{k}\left(\frac{s^2}{w_i^2}+\alpha_i\zeta_i\frac{s}{w_i}+1\right)-\prod_{i=1}^{k}\left(\frac{s^2}{w_i^2}+\zeta_i\frac{s}{w_i}+1\right)}{\prod_{i=1}^{k}\left(\frac{s^2}{w_i^2}+\alpha_i\zeta_i\frac{s}{w_i}+1\right)} \quad .\end{aligned} \tag{18}$$

From Eq. (18), there is one differentiator in the numerator of $Q(s)$, and meanwhile $Q(s)$ features a low-pass characteristic since its relative degree is one. Therefore, the $Q(s)$ is a band-pass filter. In a below example, the open-loop vibrations are shown in Fig. 8 that include multiple peak areas.

Due to three areas of energetic vibrations existing in the high frequency, $ESF(s)$ can be designed as follows

$$ESF(s)=ESF_1(s)\times ESF_2(s)\times ESF_3(s) \quad , \tag{19}$$

Where,

$$ESF_1(s)=\frac{0.000659s^2+2.567\mathrm{e}-5s+1}{0.000659s^2+0.0154s+1} \quad , \tag{20}$$

$$ESF_2(s)=\frac{2.093\mathrm{e}-4s^2+1.447\mathrm{e}-5s+1}{2.093\mathrm{e}-4s^2+0.002894s+1} \quad , \tag{21}$$

$$ESF_3(s)=\frac{5.234\mathrm{e}-5s^2+7.234\mathrm{e}-6s+1}{5.234\mathrm{e}-5s^2+7.234\mathrm{e}-4s+1} \quad . \tag{22}$$

As can be seen in Fig. 9, the 6-order notch filter shown in Eq. (19) is designed at the centered frequencies of 6 Hz, 11 Hz, and 21 Hz respectively. As a result, $Q(s)$ is a band-pass filter.

The correction results are given in Fig. 10. The closed-loop errors are 2.32 μrad RMS and 0.63 μrad RMS respectively. In the DOBC mode, the RMS errors are less than 30% of that in the original loop. Peak disturbances still appear at 6 Hz, 11Hz and 21 Hz in the PI control mode, while they disappear in the DOBC mode.

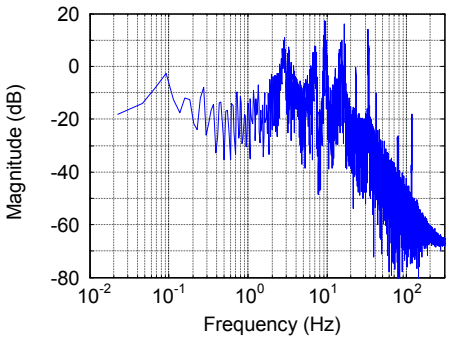

Fig. 8 | Spectra of Tip-Tilt vibrations.

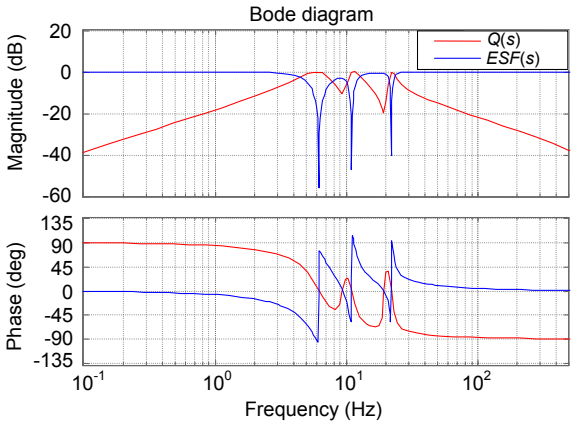

Fig. 9 | Bode response of *Q*(*s*) and *ESF*(*s*).

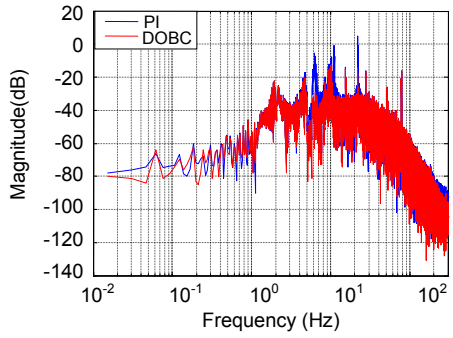

Fig. 10 | Spectra of Tip-Tilt vibrations in DOBC mode.

Repetitive control of Tip-Tilt mirror

In this chapter, a learning-type control strategy called repetitive control is applied to a new Q-filter for coping with unknown disturbances. An improved Q-filter[41] based on moving average filter is proposed to reduce the waterbed effect, which implies that additional gain amplifications can be mitigated between both periodic frequencies in comparison with conventional repetitive controller.

Q-filter design and performance analysis

The classical repetitive controller (CRC) is expressed as follows:

$$Q_{\mathrm{CRC}}(\mathrm{e}^{-sT}) = \mathrm{e}^{-sNT} q(\mathrm{e}^{-sT}, l) \quad . \tag{23}$$

A low-pass filter $q(\mathrm{e}^{-sT}, l)$ is used to block high-frequency noise and imperfect dynamics. The low-pass filter is usually designed as a zero phase filter as follows:

$$q(\mathrm{e}^{-sT}, l) = a_l \mathrm{e}^{slT} + a_{l-1}\mathrm{e}^{s(l-1)T} + \cdots a_0 + \cdots + a_{l-1} e^{-s(l-1)T} + a_l e^{-slT} \quad , \tag{24}$$

here l is a positive integer, and the coefficients meet $2(a_l + a_{l-1} + \cdots a_1) + a_0 = 1$. In the CRC mode, the extra sensitivity function is given

$$E_{\mathrm{CRC}}(\mathrm{e}^{-sT}) = 1 - \mathrm{e}^{-sNT} q(\mathrm{e}^{-sT}, l) \quad . \tag{25}$$

The maximum value of Eq. (25) is equal to 2. The magnitude response of Eq. (25) is shown in Fig. 11, showing waterbed effect at nonperiodic frequencies.

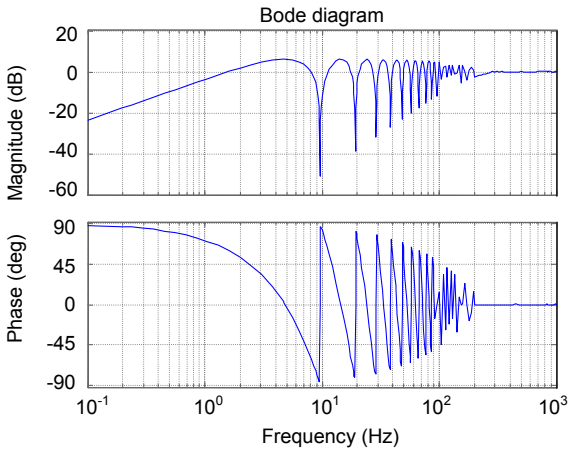

Fig. 11 | Bode response of the Eq. (25).

For relaxing disturbance amplification at the nonrepetitive frequencies, we proposed an improved repetitive controller (IRC), and the new extra sensitivity function is given below

$$E_{\mathrm{IRC}}(\mathrm{e}^{-sT}) = \frac{1 - \mathrm{e}^{-sNT} q(\mathrm{e}^{-sT}, l)}{1 - \alpha \mathrm{e}^{-sNT} q(\mathrm{e}^{-sT}, l)}, \quad \alpha \in [0,1] \quad . \tag{26}$$

Due to $q(\mathrm{e}^{-sT}, l) = q(\mathrm{e}^{sT}, l) = 1$ below the frequency of w_{c}, the $|E_{\mathrm{IRC}}(\mathrm{e}^{-sT})|^2$ is simplified as

$$\left|E_{\mathrm{IRC}}(\mathrm{e}^{-sT})\right|^2 = \frac{2 - 2\cos(w/N)}{1 + \alpha^2 - 2\alpha\cos(w/N)} \quad . \tag{27}$$

The maximum value of Eq. (27) at the frequencies of $w = \pi + 2k\pi\ (k = 0, 1, 2, \cdots)$ is 2, which implies that the worst amplification is amplified by 2. Reversely, if α is assigned a large value close to 1, the magnitude of the Eq. (27) is equal to 1. According to Bode's integral theorem, the amplification of nonperiodic disturbance can be reduced with the increase of α, while the disturbance reduction is also decreased. This phenomenon can be exhibited in Fig. 12.

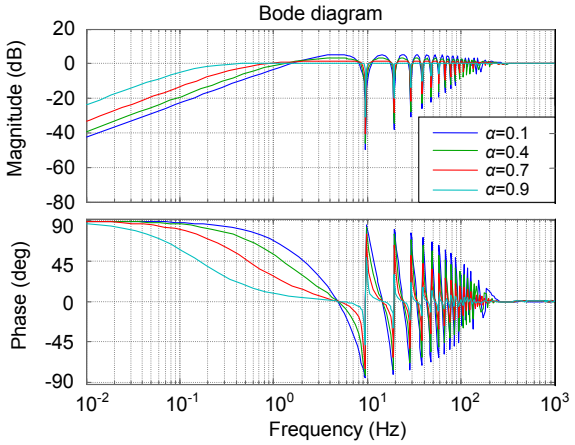

Fig.12 | Bode response of the Eq. (26).

The Q-filter of the IRC is derived below

$$Q_{\mathrm{IRC}}(\mathrm{e}^{-sT}) = 1 - E_{\mathrm{IRC}}(\mathrm{e}^{-sT}) = \frac{(1-\alpha)\mathrm{e}^{-sNT} q(\mathrm{e}^{-sT}, l)}{1 - \alpha \mathrm{e}^{-sNT} q(\mathrm{e}^{-sT}, l)} \quad . \tag{28}$$

In this section, a design example of the Tip-Tilt mirror under the condition of structural vibrations is exhibited. The sensitivity transfer functions of the Tip-Tilt mirror with IRC, CRC and I (integrator) are shown in Fig. 13. The benchmark line in blue is the closed-loop rejection with I controller, of which the rejection bandwidth is about 80 Hz, and no more than -20 dB suppression at the

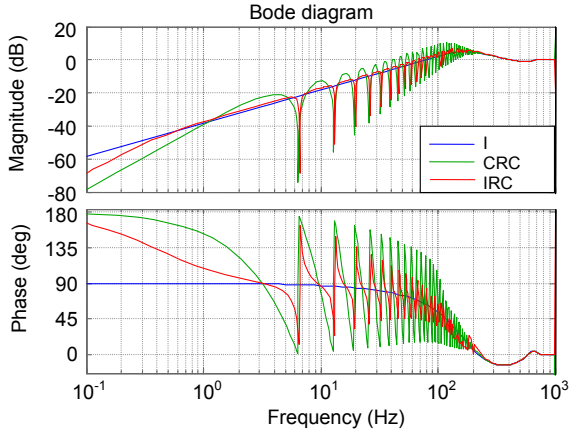

Fig. 13 | Sensitivity function responses in frequency domain.

basic frequency of repetitive disturbance. IRC rejects the vibration peak with slightly magnifications of other frequencies, leading to an efficient improvement.

Figure 14 shows the correction results in three different kinds of controllers. The resulting Tip-Tilt errors are 1.28, 0.91 and 0.66 μrad RMS respectively with I, CRC and IRC. The CRC has reduced Tip-Tilt error at the steady state, less than 72% of the original error, while in IRC mode the error is about 52% of the original error. The spectra are shown in Fig. 15 when the repetitive controllers are employed. The peak vibrations at the basic frequency of 6.6 Hz (such as 6.6 Hz, 13.2 Hz, 19.8 Hz and 26.4 Hz and so on) are significantly reduced.

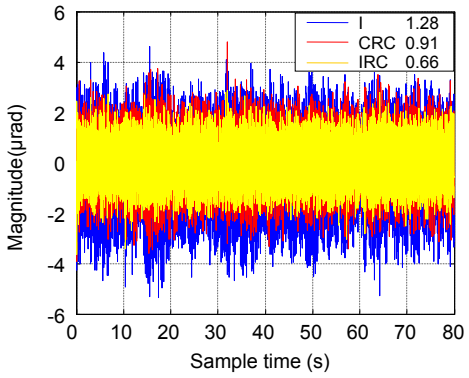

Fig. 14 | Tip-Tilt errors in different control modes.

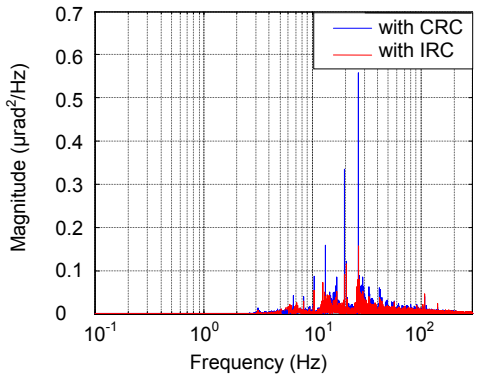

Fig. 15 | Spectra of Tip-Tilt vibrations with CRC and IRC.

Conclusion

In this paper, the control methodologies of Tip-Tilt mirror to reject structural vibrations in optical telescopes are reviewed and discussed. We focus on the survey of an error-based disturbance observer controller of the Tip-Tilt mirror. In this mode, a generalized version of 1−Q is cascaded into the original sensitivity function, and therefore the design of the Q-filter plays a vital role in the closed-loop control system of the Tip-Tilt mirror. The low-pass filter, band-pass filter and repetitive filter of the Q-filter are proposed to cope with vibrations in different frequency modes. The implementation of the proposed DOBC structure, the optimization of the control parameters and the analysis of the close-loop characteristics from the viewpoint of its practical implementation are provided in this paper. The key problem of designing the improved Q-filter is to determinate disturbance frequencies. A scanning method[42] can make sure the accuracy in detection of the interesting vibrations. The control bandwidth of the Tip-Tilt mirror is not improved with this proposed controller, but disturbance attenuation is greatly enhanced at the disturbance frequencies. Furthermore, this improved control mode cannot cause big magnifications at non-disturbance frequencies, and therefore an effective improvement of the closed-loop performance is obtained. In comparison with existed methods, this improved technique can be carried out in real time if disturbance frequencies are given. Disturbance suppression, especially beyond the Nyquist frequency may be a continuing and attractive research in the mechanical control area. Nonlinear techniques[43–46] such as sliding mode control, repetitive control, backstepping control and active disturbance rejection control are promising for further rejection performance in the high precision control system.

References

1. Chen X, Tomizuka M. Overview and new results in disturbance observer based adaptive vibration rejection with application to advanced manufacturing. *Int J Adaptive Control Signal Process* **29**, 1459–1474 (2015).
2. Shtessel Y, Edwards C, Fridman L, Levant A. *Sliding Mode Control and Observation* (Springer, New York, 2014).
3. Tomizuka M. Control methodologies for manufacturing applications. *Manuf Lett* **1**, 46–48 (2013).
4. Gao Z Q. Active disturbance rejection control: a paradigm shift in feedback control system design. In *Proceedings of 2006 American Control Conference* (IEEE, 2006); http://doi.org/10.1109/ACC.2006.1656579.
5. Han J Q. From PID to active disturbance rejection control. *IEEE Trans Ind Electron* **56**, 900–906 (2009).
6. Deng C , Tang T , Mao Y , *et al*. Enhanced Disturbance Observer Based on Acceleration Measurement for Fast Steering Mirror Systems. *IEEE Photonics Journal* **9**, 1–11(2017).
7. Lozi J, Guyon O, Jovanovic N, Singh G, Goebel S *et al*. Characterizing and mitigating vibrations for SCExAO. *Proc SPIE* **9909**, 99090J (2016).
8. Rao C H, Gu N T, Zhu L, Huang J L, Li C *et al*. 1.8-m solar telescope in China: Chinese large solar telescope. *J Astron Telescopes Instrum Syst* **1**, 024001 (2015).
9. MacMartin D G. Control challenges for extremely large telescopes. *Proc SPIE* **5054**, 275–286 (2003).
10. Gawronski W. Control and pointing challenges of large antennas and telescopes. *IEEE Trans Control Syst Technol* **15**, 276–289 (2007).
11. Petit C, Sauvage J F, Fusco T, Sevin A, Suarez M *et al*. SPHERE extreme AO control scheme: final performance assessment and on sky validation of the first auto-tuned LQG based operational system. *Proc SPIE*, **9148**, 91480O (2014).
12. MacMartin D G, Thompson H A. Vibration budget for observatory equipment. *J Astron Telesc Instrum Syst* **1**, 034005 (2015).
13. Böhm M, Pott J U, Kürster M, Sawodny O, Defrère D *et al*. Delay compensation for real time disturbance estimation at extremely large telescopes. *IEEE Trans Control Syst Technol* **25**,

1384–1393 (2017).
14. Glück M, Pott J U, Sawodny O. Piezo-actuated vibration disturbance mirror for investigating accelerometer-based tip-tilt reconstruction in large telescopes. *IFAC-PapersOnLine* **49**, 361–366 (2016).
15. Ken F, Susumu Y, Nobutaka B, Shin-ichiro S, Atsuo T *et al*. Accelerometer assisted high bandwidth control of tip-tilt mirror for precision pointing stability. In *Proceedings of IEEE on Aerospace Conference* (IEEE, 2011); http://doi.org/10.1109/AERO.2011.5747383.
16. Agapito G, Battistelli G, Mari D, Selvi D, Tesi A *et al*. Frequency based design of modal controllers for adaptive optics systems. *Opt Express* **20**, 27108–27122 (2012).
17. Muradore R, Pettazzi L, Fedrigo E. Adaptive vibration cancellation in adaptive optics: An experimental validation. In *Proceedings of 2014 European Control Conference* 2418–2423 (IEEE, 2014); http://doi.org/10.1109/ECC.2014.6862434.
18. Pettazzi L, Fedrigo E, Muradore R, Haguenauer P, Pallanca L. Improving the accuracy of interferometric measurements through adaptive vibration cancellation. In *Proceedings of 2015 IEEE Conference on Control Applications* 95–100 (IEEE, 2015); http://doi.org/10.1109/CCA.2015.7320616.
19. Yang K J, Yang P, Chen S Q, *et al*. Vibration identification based on Levenberg-Marquardt optimization for mitigation in adaptive optics systems. *Appl Opt* **57**, 2820–2826 (2018).
20. Böhm M, Pott J U, Kürster M, Sawodny O. Modeling and identification of the optical path at ELTs- a case study at the LBT. *IFAC Proc Volumes*, **46**, 249–255(2013).
21. Castro M, Escárate P, Zuñiga S, Garcés J, Guesalaga A. Closed loop for tip-tilt vibration mitigation. In *Applications of Lasers for Sensing and Free Space Communications 2015* (OSA, 2015); https://doi.org/10.1364/AOMS.2015.JT5A.28.
22. Petit C, Conan J M, Kulcsár C, Raynaud H F. Linear quadratic Gaussian control for adaptive optics and multiconjugate adaptive optics: experimental and numerical analysis. *J Opt Soc Am A* **26**, 1307–1325 (2009).
23. Radke A, Gao Z Q. A survey of state and disturbance observers for practitioners. In *Proceedings of 2006 American Control Conference* (IEEE, 2006); http://doi.org/10.1109/ACC.2006.1657545.
24. Sariyildiz E, Ohnishi K. Stability and robustness of disturbance-observer-based motion control systems. *IEEE Trans Ind Electron* **62**, 414–422 (2015).
25. Chen W H, Yang J, Guo L, Li S H. Disturbance-observer-based control and related methods-an overview. *IEEE Trans Ind Electron* **63**, 1083–1095 (2016).
26. Kim J S, Back J, Park G. Design of Q-filters for disturbance observers via BMI approach. In *Proceedings of the 14th International Conference on Control, Automation and Systems* 1197–1200 (IEEE, 2014); http://doi.org/10.1109/ICCAS.2014.6987741.
27. Zheng M H, Zhou S Y, Tomizuka M. A design methodology for disturbance observer with application to precision motion control: an H-infinity based approach. In *Proceedings of 2017 American Control Conference* 3524–3529 (IEEE, 2017); http://doi.org/10.23919/ACC.2017.7963492.
28. Tang T, Qi B, Yang T. Youla-Kucera parameterization-based optimally closed-loop control for tip-Tilt compensation. *IEEE Sens J* **18**, 6154–6160 (2018).
29. Tang T, Yang T, Qi B, Cao L, Ren G *et al*. Error-based plug-in controller of tip–tilt mirror to reject telescope's structural vibrations. *J Astron Telesc Instrum Syst* **4**, 049004 (2018).
30. Chen X, Jiang T Y, Tomizuka M. Pseudo Youla-Kucera parameterization with control of the waterbed effect for local loop shaping. *Automatica* **62**, 177–183 (2015).
31. Jiang T Y, Chen X. Transmission of signal nonsmoothness and transient improvement in add-on servo control. *IEEE Trans Control Syst Technol* **26**, 486–496 (2017).
32. Zhou K L, Wang D W, Zhang B, Wang Y G. Plug-in dual-mode-structure repetitive controller for CVCF PWM inverters. *IEEE Trans Ind Electron* **56**, 784–791 (2009).
33. Cho Y, Lai J S. Digital plug-in repetitive controller for single-phase bridgeless PFC converters. *IEEE Trans Power Electron* **28**, 165–175 (2013).
34. Chen X, Tomizuka M. New repetitive control with improved steady-state performance and accelerated transient. *IEEE Trans Control Syst Technol* **22**, 664–675 (2014).
35. Mahani N K Z, Sedigh A K, Bayat F M. Performance evaluation of non-minimum phase linear control systems with fractional order partial pole-zero cancellation. In *Proceedings of the 9th Asian Control Conference* (IEEE, 2013); http://doi.org/10.1109/ASCC.2013.6606329.
36. Stengel R F. *Optimal Control and Estimation* (Dover Publications, New York, 1994).
37. Siouris G M. Errata to an engineering approach to optimal control and estimation theory. *IEEE Aero Electron Syst Mag* **12**, 37 (1997).
38. Glück M, Pott J U, Sawodny O. Investigations of an accelerometer-based disturbance feedforward control for vibration suppression in adaptive optics of large telescopes. *Pub Astron Soc Pacific* 2017, **129**, 065001 (2017).
39. Kempf C J, Kobayashi S. Disturbance observer and feedforward design for a high-speed direct-drive positioning table. *IEEE Trans Control Syst Technol* **7**, 513–526 (1999).
40. Kim B K, Chung W K. Advanced disturbance observer design for mechanical positioning systems. *IEEE Trans Ind Electron* **50**, 1207–1216 (2003).
41. Tang T, Xu N S, Yang T, Qi B, Bao Q L. Vibration rejection of Tip-Tilt mirror using improved repetitive control. *Mech Syst Signal Process* **116**, 432–442 (2019).
42. Guesalaga A, Neichel B, O'Neal J, Guzman D. Mitigation of vibrations in adaptive optics by minimization of closed-loop residuals. *Opt Express* **21**, 10676–10696 (2013).
43. Huang Y, Xue W C. Active disturbance rejection control: Methodology and theoretical analysis. *ISA Trans* **53**, 963–976 (2014).
44. Chen W H. Disturbance observer based control for nonlinear systems. *IEEE/ASME Trans Mech* **9**, 706–710 (2004).
45. Won D, Kim W, Shin D, Chung C C. High-gain disturbance observer-based backstepping control with output tracking error constraint for electro-hydraulic systems. *IEEE Trans Control Syst Technol* **23**, 787–795 (2015).
46. Liu L P, Fu Z M, Song X N. Sliding mode control with disturbance observer for a class of nonlinear systems. *Int J Autom Comput* **9**, 487–491 (2012).

Acknowledgements

This work was in part supported by Youth Innovation Promotion Association, Chinese Academy of Sciences

Competing interests

The authors declare no competing financial interests.